

Scientific Paper

Doi: <http://dx.doi.org/10.1590/1809-4430-Eng.Agric.v42n5e20220026/2022>

STUDY ON THE EFFECT OF KEY PARAMETERS OF A FERTILISATION DEVICE ON FERTILISATION DEPTH

Liwei Guo¹, Kan Zheng^{1*}, Junfang Xia¹, Liu Jiang¹, Guoyang Liu¹

^{1*}Corresponding author. Huazhong Agricultural University/Wuhan, China.

E-mail: zhengkan@mail.hzau.edu.cn | ORCID ID: <https://orcid.org/0000-0002-6041-5609>

KEYWORDS

agricultural machinery, fertiliser particle, precision side-depth fertilisation, fertilisation depth, non-contact mechanical fertilisation.

ABSTRACT

In view of the problems of the uneven spatial distribution of particle fertiliser and unstable depths of side-deep fertilisation, caused by existing fertiliser application devices in fertile ditches, the influence of key factors of fertiliser application devices on the depth of fertilisation was studied, in combination with the agronomic characteristics of side-deep fertilisation for the direct seeding of rice in the middle and lower reaches of the Yangtze River. By analysing the incident mud process of fertiliser particles, the factors influencing the impact of mud resistance were determined. Through the theoretical and simulation analysis of the fertilisation device, it was determined that the impact distance, the impact surface radian and the fertiliser particle diameter have the greatest impact on the fertilisation depth of the device. Single factor and orthogonal tests were carried out, with three key factors as test factors and fertilisation depth as the test index. The test results revealed that the influence of the three factors on fertilisation depth follows the order of fertiliser particle diameter > impact distance > impact surface radian. With the maximum fertilisation depth as the objective, the optimal combination of the working parameters was identified as fertiliser particle diameter = 16.0 mm, impact distance = 56.5 mm, and impact surface radian = 29.6°. Furthermore, field tests were carried out in paddy fields with a water content of $37.00 \pm 2.60\%$. When the fertilisation depth was pre-set as 50 mm, the relative error between the pre-set value and actual fertilisation depth was lower than 8.8%. The fertilisation depth can meet the agronomic requirements of side deep fertilisation and the results provide an important reference for the design of a non-contact fertilisation device for direct rice seeding.

INTRODUCTION

World hunger is an overarching issue and will remain a major concern in the 21st century (Lal, 2010). As a major staple crop, rice feeds more than half of the world's population. In rice planting, the appropriate use of fertiliser can improve rice yield and vitality, inhibit weed growth and maintain soil fertility, as well as reduce the workload and production cost, so as to facilitate the sustainable development of agriculture (Yang et al., 2018; Liu et al., 2021). Precision side-depth fertilisation application technology combines precision fertilisation application with side-depth fertilisation application technology. When rice is sown, quantitative fertilisation is applied to the soil at a certain depth (fertilisation application depth 50 mm) at the side of the rice bud row (30-50 mm from the side of the seed fertilisation) and then covered by a mulching device. This method of fertilisation application is synchronous with the

sowing of the seeds and allows the base fertilisation, greening fertilisation and tiller fertilisation to be applied at once, reducing the number of operations and saving on labour input costs. The fertilisation is concentrated at a certain lateral depth from the root system of the rice seedlings, which not only avoids injury to the roots or burns to the seedlings, but also facilitates nutrient uptake by the seedlings. The fertilisation is covered by the mud, so that the drainage nutrients are not lost and fertilisation loss is reduced, thus improving the fertilisation efficiency (Wang et al., 2018a; Zhao et al., 2020; Min et al., 2021; Zhong et al., 2021; Chen et al., 2014).

Therefore, research into the technology related to precise side-deep fertiliser application devices for the direct seeding of rice in water can effectively improve the utilisation rate of chemical fertiliser, increase the income from the rice crop and reduce environmental pollution, which is of great significance to the realisation of full

¹ Huazhong Agricultural University/Wuhan, China.

Area Editor: João Paulo Arantes Rodrigues da Cunha

Received in: 2-23-2022

Accepted in: 8-8-2022

mechanisation of rice production and sustainable agricultural development. Wang et al. (2021) designed a disc ejector type side depth fertiliser application device for paddy fields and analysed the key components of the disc ejector discharger and wind feed system, to derive the important factors affecting fertiliser application performance. The fertiliser application performance of the side depth fertiliser application device was tested, and the results showed that the device discharges fertiliser with good consistency. Zuo et al. (2016) designed an air-blower side-depth precision rice fertiliser application device, which combined the theory of wind-fed fertiliser discharge with the method of side-depth precision fertiliser application control in paddy fields, and the test showed that the device had a better side-depth fertiliser application. Wang et al. (2018b) designed a side-deep fertiliser application device for paddy fields and determined the parameters affecting the fertiliser discharge performance of the fertiliser application device by designing and analysing the key components, the fertiliser discharger and the pneumatic conveyance system. The discharge performance of the fertiliser application device was optimised and verified through bench tests, to achieve the purpose of quantitative fertiliser supply and side-deep fertiliser application. Dong et al. (2019) conducted a design study on the intermittent fixed-point precision rice side-depth fertilisation method and device, which was capable of fixed-point precision fertilisation at a set target fertilisation amount; the fertilisation effect met the requirement of side-depth fertilisation. Wan et al. (2020) designed an inter-row roller type cavity application and fertiliser discharge device and, based on Abaqus (to establish a cavity-forming kinetic model), the cavity application and fertiliser discharge device was analysed for cavity formation performance and cavity tying pressure. The tests showed that the device had a better cavity tying effect and better stability of fertiliser application depth. Wang et al. (2020; 2019) designed a pneumatic wheat precision seed-dropping device, which can place wheat seed grains in clean soil with high speed and precision by pneumatic acceleration. The device can place seed grains discharged from a precision seed discharger in a clean seed bed after tillage with high speed and precision by pneumatic acceleration and can achieve the fixed depth spot sowing of seed grains. These devices work well in precision fertilisation or side-deep fertilisation, but they do not combine precision fertilisation and side-deep fertilisation well. There are still problems with

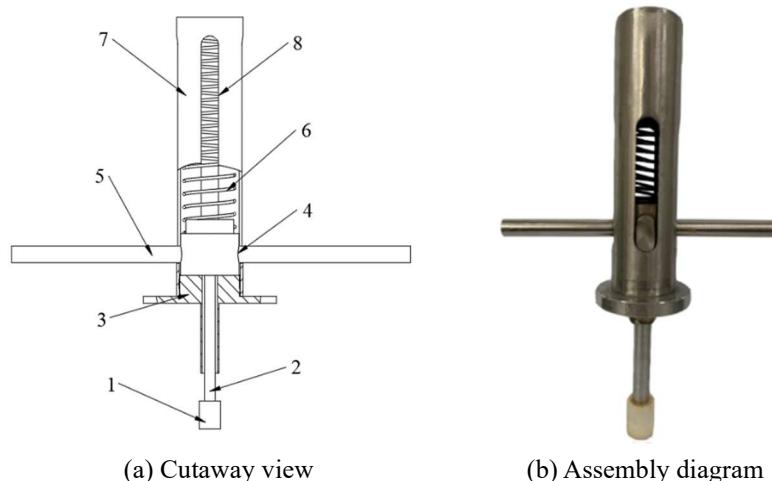
the uneven spatial distribution of particle fertiliser in the fertiliser ditch and unstable depths of side deep fertilisation still exist.

In view of these problems, the influence of key factors of fertilisation devices on fertilisation depth was studied on the basis of the physical and mechanical parameters of self-made particle fertiliser, taking into account the agronomic characteristics of precise and side-deep fertilisation, with the aim of improving the stability of the depth of side-deep fertilisation in the fertilisation device. The key factors affecting the fertilisation depth were determined by analysing the impact resistance of fertiliser particles on the mud. In addition, the key parameters of the device were tested on the bench to determine the optimal combination. Finally, field tests were conducted to verify the performance of the optimised device. The findings provide a reference for the development of a fertilisation device to be used in direct rice seeding.

Structure and working principle of the non-contact fertilisation device

Structure of the non-contact fertilisation device

The structure of the non-contact fertilisation device is shown in Figure 1. The device is mainly composed of a shell, firing pin, guide rail, push rod, firing pin cap and spring. According to the agronomic requirements of rice water direct seeding and the later design of the device, the diameter of the shell was set at 40 mm, the wall thickness was set at 2 mm, and the length was set at 160 mm. There are four grooved push rod guides (120 mm × 12 mm) on the shell, which allow the push rod to move up and down. On this basis, the diameter of the spring was set at 30 mm and the spring wire diameter was set at 2 mm. In the pre-test, when the compression of the spring was about 100 mm, the fertilisation depth could reach about 50 mm, which can meet the requirements of shallow fertilisation. Therefore, a spring with a wire diameter × outside diameter × length of 2 mm × 30 mm × 160 mm was finally selected. From the spring stiffness formula, the spring elasticity coefficient $k = 0.477$ (N/mm). The firing pin is 100 mm in length and 10 mm in diameter. A through-hole is set at the upper end of the firing pin for the insertion of the push rod. The firing pin can move up and down along the guide rail. The lower end of the firing pin is connected to a cap, 3D printed with white resin material.



1. Firing pin cap 2. Firing pin 3. Firing pin guide 4. Hole 5. Putter 6. Spring 7. Shell 8. Push rod guide

FIGURE 1. Structural diagram of the non-contact fertilisation device.

Operational principle

When the fertilisation device works, the firing pin is perpendicular to the ground in the paddy field. The same force is separately given to both ends of the pusher, so that the pusher moves upward along the pusher guide on the housing, driving the firing pin to move upward and compress the spring; the elastic potential energy increases during the compression process. When the spring is compressed to 100 mm, the force is stopped. When the particle fertiliser movement to the firing pin directly below, release the push rod, under the action of the spring elastic potential energy, drives the firing pin to hit the particle fertiliser, the elastic potential energy of the spring into the kinetic energy of the particle fertiliser, the particle fertiliser into the soil of the paddy field at a certain depth.

ANALYSIS OF THE KEY PARAMETERS

Resistance of mud to fertiliser particles

The non-contact fertilisation device is intended to be used in paddy field fertilisation. The resistance of the paddy field mud to the fertiliser particle greatly determines the entering speed of fertiliser particles into the soil and ultimately affects the fertilisation depth. Therefore, by analysing the impacting process of fertiliser particles on the mud, the factors affecting the resistance of fertiliser particles can be determined (May & Woodhull, 1948; Shen et al., 2022; Jalalisendi & Porfiri, 2018; Wen et al., 2020; Sui et al., 2021). After the fertiliser particle is impacted, it enters the mud and moves from OAA' to $O'BB'$, as shown in Figure 2. The radius edge AA' is segmented and any two adjacent points A_i and A_{i+1} form a micro boundary A_iA_{i+1} , and the B_iB_{i+1} radian is the expanded boundary of A_iA_{i+1} .

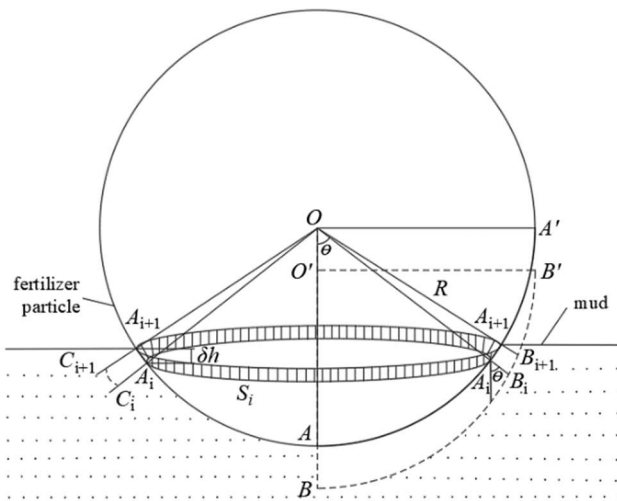


FIGURE 2. Schematic diagram of the fertiliser particle impacting the mud.

Note: O and O' are the centre of the fertiliser particle; AA' and BB' are the radius edges of fertiliser particles; A_iA_{i+1} is the boundary formed by any two adjacent points A_i and A_{i+1} ; B_iB_{i+1} is the boundary formed by any two adjacent points B_i and B_{i+1} ; C_iC_{i+1} is the perturbation wave surface generated by the forced motion of the fluid under the action of the element boundary A_iA_{i+1} ; S_i is the spatial position of the element plane represented by A_iA_{i+1} ; θ is the angle between OA_i and OA ; R is the radius of fertiliser particles, mm; and δh is the projection height of the infinite element boundary A_iA_{i+1} in the vertical direction, mm.

The spatial position of the micro surface represented by A_iA_{i+1} is the shaded part S_i in Figure 2. The area of S_i on the element surface dS_i is

$$dS_i = 2\pi\delta h R \cos \theta \tag{1}$$

Where:

dS_i is the area of S_i on the micro-element surface, mm^2 ;

δh is the vertical projection height of the element boundary A_iA_{i+1} , mm;

θ is the included angle of OA_i and OA , and

R is the fertiliser particle radius, mm.

It is assumed that the equivalent expansion rate of A_iA_{i+1} surface fluid is v_i ; the disturbed wave surface generated by forced fluid motion under the action of A_iA_{i+1} on the boundary element after δt time is C_iC_{i+1} ; the expansion velocity of the wave surface is c ; and the fluid behind the wave surface C_iC_{i+1} is in an undisturbed state, with a velocity of 0. According to the elastic theory, the propagation velocity of a wave is sound velocity c . At this moment, the distance between the wave surface and the centre O of the moving fertiliser particle is R_{ci} . After δt , the fluid mass in the newly disturbed region is δm_θ . When δt is small enough, the fluid velocity in the newly disturbed region can be considered as being equal, so the average fluid velocity in the region is v_{ci} . Assuming that the force acting on δm_θ is F_{ci} in δt time, the average value is \bar{F}_{ci} . According to the momentum theorem, \bar{F}_{ci} is

$$\begin{cases} R_{ci} = R + (c - v_i)(t - t_i) \\ \delta m_\theta = \frac{dS_i \rho R_{ci}^2 (c - v_i) \delta t}{R^2} \\ v_{ci} = \frac{R^2}{R_{ci}^2} v_i = \frac{R^2}{R_{ci}^2} V_p \cos \theta \\ \bar{F}_{ci} = \frac{\delta M_\theta}{\delta t \cos \theta} = \frac{\delta m_\theta v_{ci} \cos \theta}{\delta t \cos \theta} = \frac{\delta m_\theta v_{ci}}{\delta t} \end{cases} \tag{2}$$

In [eq. (2)], R_{ci} is the distance between the wave surface and the centre O of the moving fertiliser particle, mm; c is sound speed, m/s; v_i is the equivalent expansion rate of the fluid, mm/s; t is the system time, s; t_i is the water contact time of micro boundary A_iA_{i+1} , s; δm_θ is the fluid mass in the newly disturbed region, g; ρ is the mud density, kg/m^3 ; v_{ci} is the average velocity of fluid, mm/s; V_p is the moving velocity of the fertiliser particle along the gravity direction, mm/s; and \bar{F}_{ci} is the mean value of the force acting on δm_θ .

At the micro level, F_{ci} is variable, but the displacement velocity of the interface is v_{ci} , and then the work δW_i of the force F_{ci} at δt time can be calculated by using the average force. According to the law of energy, the kinetic energy loss dE of the fertiliser particle should be equal to the sum of the work done by each element boundary

to the fluid at δt time. Then, at time δt , the resultant external force received by the fertiliser particle, that is, the impact resistance of the mud F , is

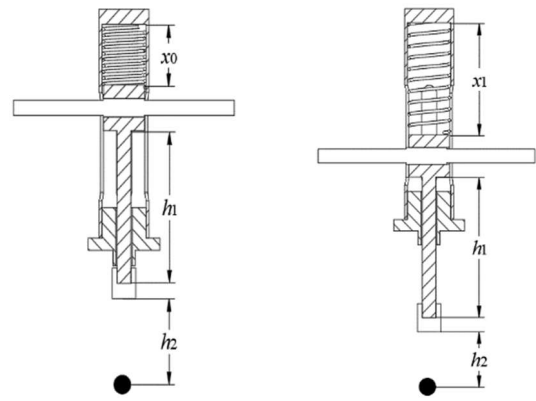
$$\begin{cases} dE = \sum_{i=1}^n \delta W_i = \sum_{i=1}^n \bar{F}_{ci} v_{ci} \delta t \\ F = \frac{dE}{dL} = \frac{dE}{V_p \delta t} = \sum_{i=1}^n \frac{dS_i R^2 V_p (c - v_i) \rho \cos^2 \theta}{R_{ci}^2} \end{cases} \quad (3)$$

According to the formula of the impact resistance, in the process that the fertiliser particle impacts the mud, many factors affect the impact resistance, particularly the radius R of the fertiliser particle and the velocity V_p of impacting. The projection δh of the element boundary $A_i A_{i+1}$ in the vertical direction and the angle θ between OA_i and OA , have less variation during the impact of the fertiliser particle on the mud. The water contact time t_i of element boundary $A_i A_{i+1}$ and the system time t show little change during the impact process and, thus, have little influence on the impact resistance. The wave surface expansion velocity c and mud density ρ are fixed values. To sum up, among these factors, the fertiliser particle diameter and impacting speed have a more significant and complex influence on the impact resistance. In the vertical entry of fertiliser particles into the mud, greater impact resistance will lead to a faster decrease in the kinetic energy of the fertiliser particle, resulting in a shallower fertilisation depth.

Kinetic energy analysis of the fertiliser particle applied by the device

Effect of the device structure on the kinetic energy of the fertiliser particle

According to the formula of impact resistance, the kinetic energy of the fertiliser particle after impact will affect the impact resistance which will, in turn, affect the fertilisation depth. Therefore, by analysing the structure of the non-contact fertilisation device, the factors affecting the kinetic energy of fertiliser particles were determined. During the operation of the device, the spring is released from the compressed state to drive the firing pin to impact the fertiliser particle. During the impact, the spring force does positive work and the elastic potential energy of the spring is converted into the kinetic energy of the fertiliser particle (Wu et al., 2020; May, 1952).



(a) Spring length is x_0 (b) Spring length is x_1

FIGURE 3. Changes in spring length during compression and release.

As shown in Figure 3(a), the push rod moves to the top along the guide rail and the spring is compressed from the original length to x_0 . At this time, the compression amount of the spring is x_2 and the elastic potential energy is E_0 . As shown in Figure 3(b), during the impact of the firing pin on the fertiliser particle, the spring length x_1 becomes longer and the compression amount of the spring becomes smaller. At this time, the compression amount of the spring is x_3 and the elastic potential energy is E_1 . The reduction of elastic potential energy E_p in the process of the spring length changing from x_0 to x_1 is

$$\begin{cases} x_2 = 160 - x_0 \\ E_0 = \frac{1}{2} k x_2^2 \\ x_3 = 160 - x_1 \\ E_1 = \frac{1}{2} k x_3^2 \\ E_p = E_0 - E_1 = \frac{1}{2} k x_2^2 - \frac{1}{2} k x_3^2 \end{cases} \quad (4)$$

According to the above analysis and [eq. (4)], when the push rod is released, a greater vertical distance h_2 between the firing pin and the fertiliser particle will lead to smaller spring compression x_3 and, correspondingly, a higher E_p . When the firing pin hits the fertiliser particle, E_p is converted into the kinetic energy of the fertiliser particle.

$$Ft = P - P_0 = mv - mv_0 \quad (5)$$

According to the momentum theorem and [eq. (5)] of quantitative theorem, the velocity of a fertiliser particle after impact is associated with both the force F on the fertiliser particle and the contact time t between the fertiliser particle and firing pin. The force F is related to E_p . In other words, it is related to the vertical distance h_2 between the fertiliser particle and the firing pin, which is referred to as the impact distance. Together, the impact distance and impact time determine the kinetic energy of the fertiliser particle, affecting the impact resistance and, finally, determining fertilisation depth.

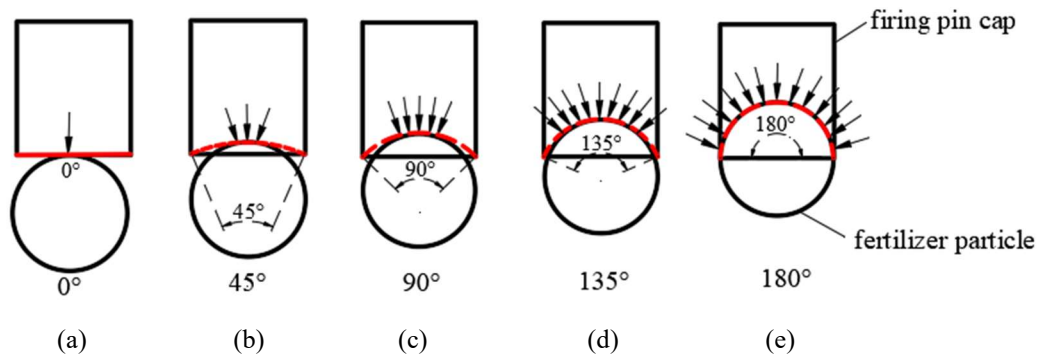


FIGURE 4. Distribution diagram of force on different surface radians.

The designed device is intended to be used in a paddy field. To ensure the accuracy of fertilisation and reduce the influence of uncertain factors, the vertical distance between the fertiliser particle and water surface should not be too high; otherwise, the mud and water may be easily splashed on the fertiliser particles, making the fertiliser particles soft and wetted, which may then become deformed and, even, broken by the strong impact force of the firing pin. The red dotted line in Figure 4 indicates the contact surface between the fertiliser particle and the bottom of the firing pin cap; the corresponding radian is called the impact surface radian. When the impact surface radian is 0° , the firing pin cap and fertiliser particle are in a point contact and the force of the firing pin on the fertiliser particle is concentrated, which may cause great damage to the internal structure of the fertiliser particle. This may result in the deformation, higher maximum cross section and even breaking of the fertiliser particle, as well as having an effect on the kinetic energy of the fertiliser particle, including fertilisation depth. When the impact surface radian is changed from 0° to 180° , the firing pin cap is in a surface contact state with the fertiliser particle, and a larger radian represents a greater contact area. This surface contact mode does relatively little damage to the internal structure of the fertiliser particle, reducing the impact on the kinetic energy of the fertiliser particle into the soil, and maintaining a stable fertilisation depth.

In conclusion, the impact distance corresponds to the impact time during the whole impact process. Since it is difficult to measure the impact time, the impact distance was selected as a factor to be tested, in order to reduce the testing errors. Previous analysis has indicated that the impact

distance and impact surface radian have a great effect on the kinetic energy of the fertiliser particle.

Effect of particle diameter on the kinetic energy of the fertiliser particle

According to the formula of impact resistance, the resistance is different for fertiliser particles with different diameters when being impacted into the mud. A larger diameter will lead to greater resistance, and the kinetic energy is also different for fertiliser particles with different diameters. Therefore, through the finite element simulation software, the simulation is divided into two stages: the stage when the cam compresses the push rod to make the striker store energy and the stage when the striker impacts the particle fertiliser. The change in the kinetic energy of the particle fertiliser, with different diameters after impact, was analysed to determine the effect of particle fertiliser diameter on the kinetic energy of the particle fertiliser. The non-contact fertilisation device requires self-made fertiliser particles, and different amounts of basal fertiliser are required by rice in different areas. According to the agronomic requirements of rice planting (namely a row distance of 25 cm and a plant distance of 14 cm), the basal fertiliser required by each hill of rice was calculated to be 2.4 ± 0.8 g. Then, based on the measured fertiliser particle density of 1120 kg/m^3 , the volume of fertiliser particles required for each rice hill could be obtained. Combined with the volume formula, the fertiliser particles with diameters of 16 mm, 14 mm, 12 mm, 10 mm and 8 mm were made for the fertilisation of 1 (2.4 g), 2 (3.2 g), 3 (3.0 g), 4 (2.3 g) and 5 (1.6 g) particles, respectively.

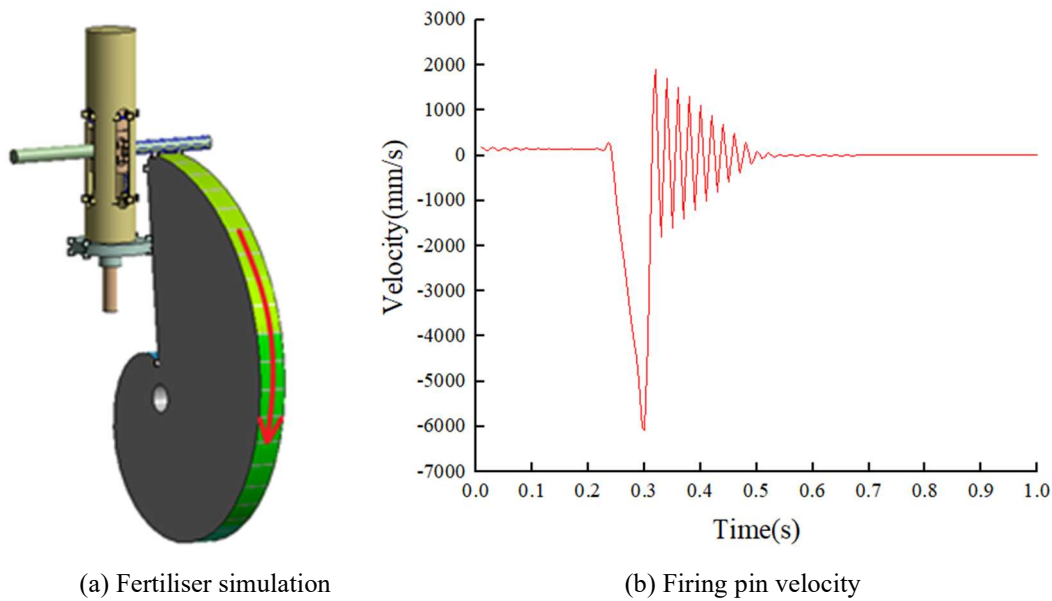


FIGURE 5. Simulation of the non-contact fertilisation device and firing pin velocity diagram.

Finite element simulation software (ANSYS Workbench) was used to simulate the impact process of fertiliser particles and explore the influence of particle diameter on the fertilisation depth. As shown in Figure 5, the Transient Structural module in ANSYS Workbench was used to simulate the motion of the spring from compression to release, and the changes in velocity of the firing pin were recorded during the whole process. During the simulation process, the cam rotates clockwise from the static state, to compress the spring. The cam base circle diameter is 100 mm, the maximum cam travel is 200 mm, and the position of the adjustment device in relation to the cam. When the cam rotates to the position shown in Figure 5(a), which is the furthest position of the push rod from the cam axis, it is the critical state of contact between the cam and the push rod,

and the spring is compressed to 100 mm. When the cam continues to rotate, the push rod breaks away from the cam. Under the action of the spring, the firing pin is driven to move downward along the guide rail until it contacts the bottom and stops moving.

Figure 5(b) shows the changes in the velocity of the firing pin in the first second of the simulation. In the first 0.25 s, the firing pin moves upward at a steady speed under driving by the cam; between 0.25 s and 0.3 s, the push rod breaks away from the cam, and under the action of the spring, the firing pin moves rapidly downward. The fastest speed of 6075 mm/s appears at 0.3 s; between 0.3–1.0s, the firing pin moves up and down under the driving of the spring, and the speed slowly tends to 0 mm/s.

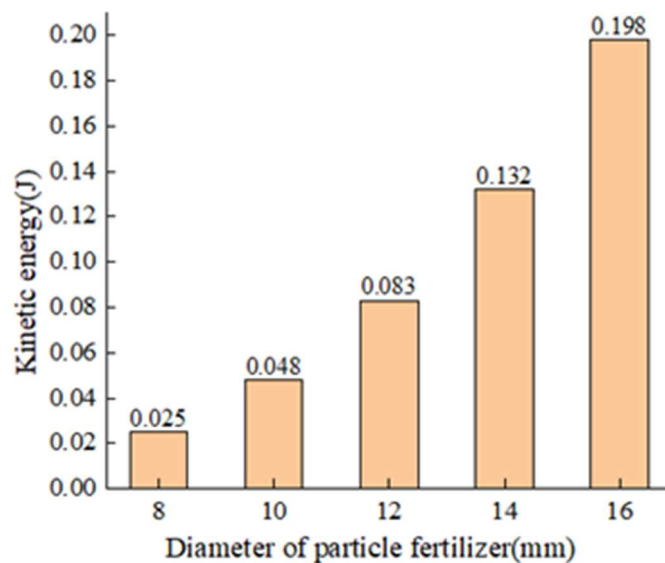


FIGURE 6. Kinetic energy of fertiliser particles with different diameters.

The Explicit Dynamics module in ANSYS Workbench was used to simplify the structure of the non-contact fertilisation device and simulate the fertilisation process. In the simulation, the firing pin is made of structural steel with a density of 7850 kg/m^3 , Poisson's ratio of 0.3 and Young's modulus of $2 \times 10^{11} \text{ Pa}$. The fertiliser particles were made into 16, 14, 12, 10 and 8 mm diameter particles, with a density of 1120 kg/m^3 , Poisson's ratio of 0.25, and Young's modulus of $7 \times 10^7 \text{ Pa}$. In the simulation, the firing pin hits the fertiliser particle at a speed of 6075 mm/s, namely the speed of the firing pin when moving to the lowest end in Figure 5(a). The kinetic energy of the fertiliser particles with different diameters after the impact was recorded are shown in Figure 6. Under the same impact force, the kinetic energy of impact obviously increases with increasing fertiliser particle diameter. According to the formula of impact resistance, an increase in fertiliser particle diameter will increase the mud resistance and then decrease the fertilisation depth but, at the same time, it will increase the kinetic energy of the fertiliser particle and increase the fertilisation depth. Therefore, the fertiliser particle diameter has a dual effect on the fertilisation depth.

MATERIAL AND METHODS

Test materials

The testing was carried out in the Laboratory of Modern Agricultural Engineering, Huazhong Agricultural University, in May 2021. Soil samples were taken from the test field ($114^{\circ}32'28''\text{E}$, $30^{\circ}49'23''\text{N}$) of the Crop Research Institute of Hubei Academy of Agricultural Sciences. The soil type was clay loam, by the five-point sampling method. The samples were collected from the 0~5 cm tillage layer, with the removal of surface rice stubble and weeds before the sampling. The sampling process and sample preparation were carried out in accordance with the standard for

geotechnical test methods GB/T 50123-2019. After natural air drying and the removal of impurities, the soil samples were loaded into a self-made square soil trough ($340 \text{ mm} \times 190 \text{ mm} \times 140 \text{ mm}$) for further testing. During the tests, the soil moisture content of the prepared soil samples was $37.00 \pm 1.00\%$, and the soil bulk density was 1.23 g/cm^3 . The fertiliser particles used in the test were self-made. A Stanley upgraded fourth element fertiliser, with a nitrogen:phosphorus:potassium ratio of 18: 18: 8, was crushed into powder, and then added to a compound fertiliser granulation binder at (3~5) kg/t. After mixing with an appropriate amount of water, it was extruded with a self-made mould and blow dried. Taking self-made particle fertiliser as a research object, 100 grains were randomly selected and their triaxial dimensions were measured with vernier callipers. The average value was obtained. The spherical rate of self-made particle fertiliser was 98.22% and its shape was similar to that of a spherical body by formula. The density of self-made particle fertiliser was about 1120 kg/m^3 , measured by the drainage method. The maximum load of the self-made fertiliser particles was about 96 N, as measured by a TMS-Pro texture analyser with an accuracy of $\pm 1\%$. The moisture content was about 12.40%, as determined by using a SDH-1202 rapid halogen moisture tester with an accuracy of 0.01%.

Testing apparatus

The testing of the non-contact fertilisation device was carried out with a self-made test bench. As shown in Figure 7, the test bench is mainly composed of a bench, the non-contact fertilisation device and a supporting plate. The framework was made of aluminium tubing. The pallet is $660 \text{ mm} \times 200 \text{ mm} \times 10 \text{ mm}$ cardboard with a round hole (30 mm diameter) in the centre, to hold the fertiliser particle. The pallet is adhered to the aluminium tube by adhesive tape. The non-contact fertilisation device is fixed on the frame by two aluminium tubes.



1. Bench 2. Pallet 3. Experimental soil 4. Hairy round holes 5. non-contact fertilisation device

FIGURE 7. Test bench for the non-contact fertilisation device.

Test method

Before the test, fertiliser particles were placed in the hairy round hole in the centre of the support plate and soil was directly placed below this, at a distance of 200 mm. The

firing pin of the fertilisation device was located just above the fertiliser particle. During the test, the push rod was pushed to move upward along the guide rail and released when the spring was compressed by 100 mm. Under the action of the spring force, the firing pin was driven to impact

the fertiliser particle into the soil. The measurement method of the fertilisation depth is shown in Figure 8. A ruler was placed horizontally on the square trough, and a light straw was inserted into the hole formed by the fertiliser particle. The contact position O between the ruler and the straw was then marked. The distance A between the bottom of the straw and O was measured with digital display electronic vernier callipers (precision of 0.01 mm). Finally, the fertilisation depth was obtained by subtracting the vertical distance B between the ruler and the soil plane from A and then adding the fertiliser particle radius R . In order to ensure reliability, the test was repeated five times at each level of each factor, and the average value was taken as the fertilisation depth at this level.

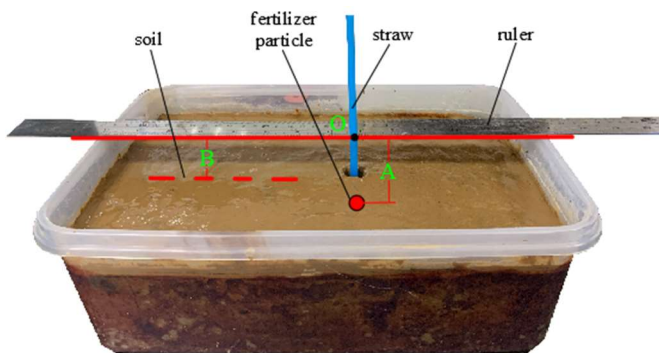


FIGURE 8. Schematic diagram of fertilisation depth measurement.

TEST RESULTS AND ANALYSIS

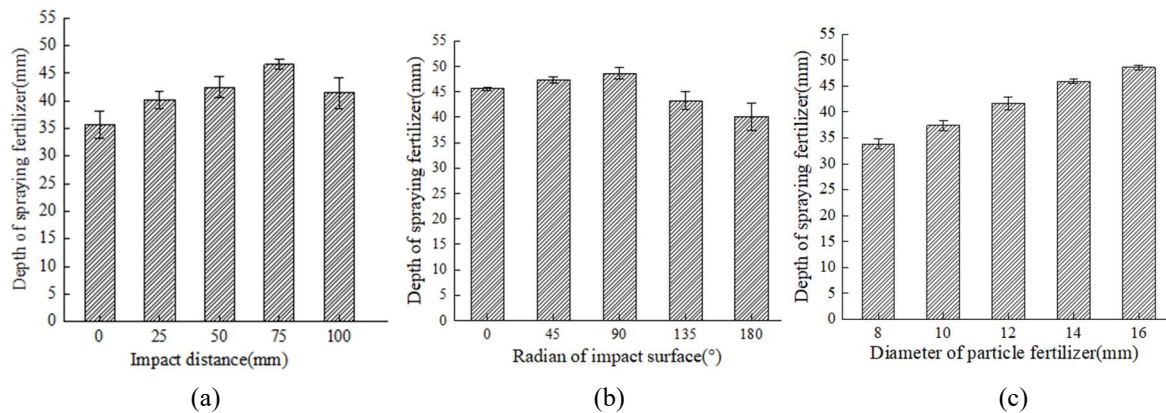
Single-factor test

According to the above analysis, impact distance, impact surface radian and fertiliser particle diameter were selected as the test factors. The impact distance was set at five levels: 0, $1/4 h_1$, $1/2 h_1$, $3/4 h_1$ and h_1 to study its effect on the fertilisation depth, where h_1 is the length of the firing pin (100 mm). The impact surface radian of $0\sim 180^\circ$ was also divided into five levels, to study its influence on the fertilisation depth. Similarly, the fertiliser particle diameter was divided into five levels, from 16 mm to 8 mm, to study its influence. The test factors and levels are shown in Table 1.

TABLE 1. Factors and levels of single-factor tests.

Levels	Factors		
	Impact distance $A/(mm)$	Impact surface radian $B/(\circ)$	Fertiliser particle diameter $C/(mm)$
1	0	0	8
2	25	45	10
3	50	90	12
4	75	135	14
5	100	180	16

In order to determine the influence of impact distance, impact surface radian and fertiliser particle diameter on the fertilisation depth, single-factor tests were carried out with the fertilisation depth as the test index, and the results are shown in Figure 9.



(a, b and c) Influence of impact distance, impact surface radian, and fertiliser particle diameter on the fertilisation depth, respectively.

FIGURE 9. Results of the single-factor tests.

When the fertiliser particle diameter is 16 mm, only one fertiliser particle is required for each rice hill. Therefore, the testing of impact distance was carried out at five levels with a fertiliser particle diameter of 16 mm and impact surface radian of 90° . The test was repeated five times for each level and each test involved one fertiliser particle. The test results are shown in Figure 9(a). It can be seen that the fertilisation depth first increases with increasing impact distance, from 0 to 75 mm, and then decreases with increasing impact distance, from 75 mm to 100 mm. The deepest depth (46.56 mm) was observed at the impact distance of about 75 mm, with an error of only 0.86. The data are highly reliable, but the fertilisation depth does not exceed 50 mm when the impact distance is 75 mm. When the impact distance ranges from 50 to 100 mm, the

fertilisation depth is the deepest. Therefore, it can be speculated that there must be an optimal impact distance in this interval.

Furthermore, the testing of impact surface radian was carried out at five levels with an impact distance of 50 mm and fertiliser particle diameter of 16 mm. The test was repeated five times for each level, and each test involved one fertiliser particle. The results are shown in Figure 9(b). It can be seen that, when the impact surface radian increases from 0° to 90° , the fertilisation depth shows a slightly rising trend; with the impact surface radian increasing from 90° to 180° , the fertilisation depth shows an obvious decreasing trend. When the impact surface radian is 180° , the fertilisation depth is the shallowest (40.15 mm), with an error of 2.67. In the test, with increasing impact surface radian, it is difficult

for the radian surface of the firing pin cap to accurately target the fertiliser particle. As shown in Figure 4, when the impact surface radian is 180°, the impact position will be uncertain, which makes it is easier to deflect the fertiliser particle and affect the fertilisation position and depth. Therefore, the impact surface radian within 0°~90° can reduce the error caused by uncertain impact position and contribute to greater fertilisation depth.

Finally, the testing of fertiliser particle diameter was carried out at five levels with an impact distance of 50 mm and impact surface radian of 90°. The test was repeated five times for each level. The results are shown in Figure 9(c). It can be seen that, with increasing fertiliser particle diameter, the fertilisation depth increases, and the error at each level does not exceed 1.19, indicating that the test data are more reliable. When the fertiliser particle diameter is 16 mm, the fertilisation depth is the deepest (48.56) mm, which also

does not exceed 50.00 mm. When the fertiliser particle diameter is 8 mm and 10 mm, the fertilisation depth is shallower, but neither exceeds 40 mm. Therefore, the fertiliser particle diameter ranging from 12 mm to 16 mm may bring about the deepest fertilisation depth.

Based on these test results, a three-factor and three-level orthogonal test was carried out, with the fertilisation depth *Y* as the test index. The upper, zero and lower levels of the impact distance, impact surface radian and fertiliser particle diameter were set at 100, 75 and 50 mm, 90°, 45° and 0°, and 16, 14 and 12 mm, respectively. There were a total of 17 groups of tests, and each group of tests was repeated five times to obtain the average value.

Orthogonal test

Test results and analysis of variance

TABLE 2. Design and results of Box-Behnken test.

No.	Factors			Fertilisation depth <i>Y</i> /(mm)
	Impact distance <i>A</i> /(mm)	Impact surface radian <i>B</i> /(°)	Fertiliser particle diameter <i>C</i> /(mm)	
1	0	0	0	46.0
2	0	-1	-1	38.7
3	1	-1	0	42.0
4	-1	1	0	47.0
5	1	0	1	48.0
6	0	1	1	49.7
7	0	1	-1	42.7
8	0	0	0	45.7
9	1	0	-1	37.3
10	0	0	0	45.0
11	-1	0	1	50.3
12	0	0	0	45.3
13	0	-1	1	49.3
14	0	0	0	45.7
15	1	1	0	42.3
16	-1	0	-1	42.0
17	-1	-1	0	46.3

The Box-Behnken test program and results are shown in Table 2. The Design-Expert 10 software was used to perform significance and variance analysis on the test results in Table 2, and the results are presented in Table 3. The regression equation significance is $P < 0.01$, indicating that the model is extremely significant, and the lack-of-fit term $P = 0.0826 > 0.05$, indicating that the equation has a high degree of fit and no obvious lack of fit. Therefore, the model is established. The value of *F* in Table 3 reveals that the influence on the fertilisation depth follows the order of

fertiliser particle diameter (*C*) > impact distance (*A*) > impact surface radian (*B*). The analysis of each item shows that *A* and *C* have extremely significant effects on the fertilisation depth, and *B*, *BC* and *A*² have significant effects. When excluding the remaining insignificant terms, the regression equation of the fertilisation depth *Y* can be obtained as follows:

$$Y = 5.5600 + 0.0232A + 0.1714B + 3.3775C - 0.0100BC - 0.0015A^2 \quad (6)$$

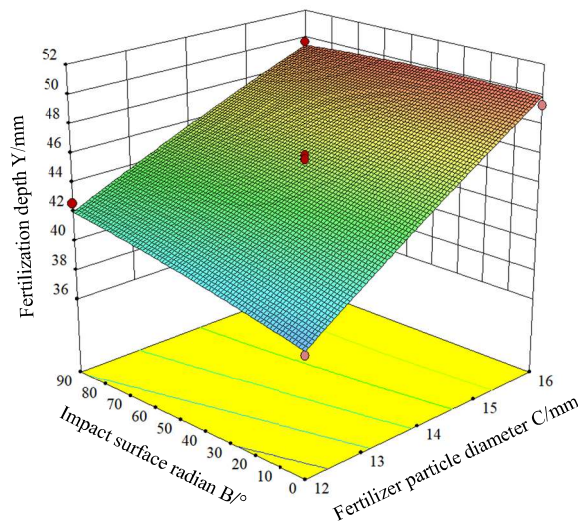
TABLE 3. Results of variance analysis.

Variation source	Sum of squares	Degree of freedom	Mean square	F value	P value
Model	212.02	9	23.56	58.85	<0.00010**
A	32.00	1	32.00	79.94	<0.00010**
B	3.65	1	3.65	9.11	0.01950*
C	167.45	1	167.45	418.31	<0.00010**
AB	0.04	1	0.04	0.10	0.76110
AC	1.44	1	1.44	3.60	0.09970
BC	3.24	1	3.24	8.09	0.02490*
A ²	3.56	1	3.56	8.90	0.02040*
B ²	0.20	1	0.20	0.51	0.49860
C ²	0.20	1	0.20	0.51	0.49860
Residual	2.80	7	0.40		
Misfit term	2.19	3	0.73	4.77	0.08260
Pure error	0.61	4	0.15		
Sum	214.82	16			

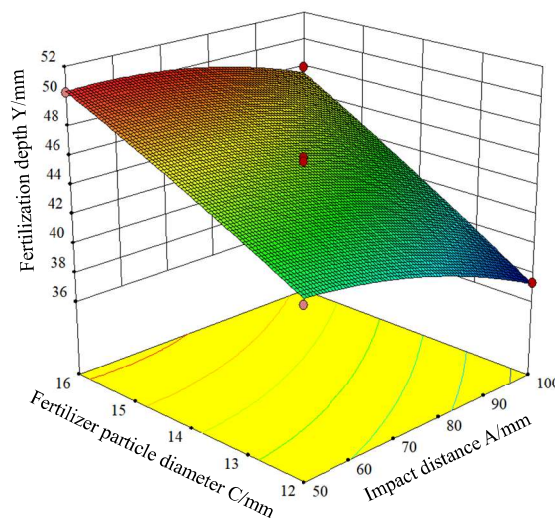
Note: * represents significant influence ($P < 0.05$), and ** represents extremely significant influence ($P < 0.01$).

Influence of factor interaction on the fertilisation depth

The influence of factor interaction on the fertilisation depth is shown in Figure 10. The significance analysis of the regression model reveals that the interaction between B and C has a significant effect, while that between A and B , or between A and C , was not significant. Figure 10a shows that when A is zero and B is constant, the fertilisation depth increases with increasing C ; when A is zero and C is between 12~14 mm, the fertilisation depth increases with increasing B ; and when A is zero and C is between 14~16 mm, the fertilisation depth decreases with increasing B .



$$Y = f(0, B, C)$$



$$Y = f(A, 0, C)$$

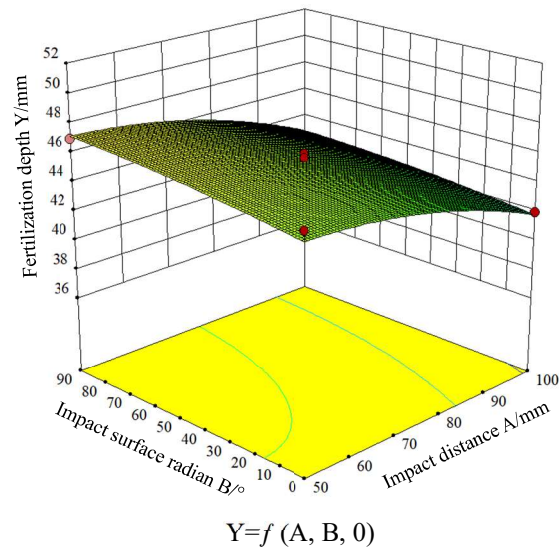


FIGURE 10. Influence of different factors on the test indices

Determination of optimal parameters

To obtain the optimal structure and working parameters of the non-contact fertilisation device, the maximum value of the objective function was obtained with the Design-Expert software, according to the actual operating conditions and work requirements, with the regression model as the objective function and the solved parameters as the constraint conditions. The optimisation objective function and constraint conditions are:

$$\begin{cases} \max Y(A, B, C) \\ \text{s.t.} \begin{cases} 50\text{mm} \leq A \leq 100\text{mm} \\ 0^\circ \leq B \leq 90^\circ \\ 12\text{mm} \leq C \leq 16\text{mm} \end{cases} \end{cases} \quad (7)$$

The objective function was solved optimally according to the constraints, and the optimal parameter combination was obtained as fertiliser particle diameter = 16.0 mm, impact distance = 56.5 mm, and impact surface radian = 29.6°.

FIELD VALIDATION TESTS

Test conditions

In order to test the performance of the non-contact fertilisation device in a real paddy field environment, a field test was conducted on May 29, 2021 in the Modern Agricultural Science and Technology Test Base of Huazhong Agricultural University (30°28'N, 114°21'E). The soil type was clay loam, the soil moisture content was 37.00 ± 2.60%, and the soil bulk density was 1.24 ± 0.30 g/cm³. Before the test, the field was treated by rotary tillage, with a pulper, and left to stand, prior to field testing. The test equipment was the test bench design described above. The test instruments mainly comprised a ruler, a level, and digital display electronic vernier callipers, with an accuracy of 0.01 mm. The test material was self-made fertiliser particles with a diameter of 16 mm.



FIGURE 11. Field test site.

Test method

The testing was carried out on a good flat area of 30 m × 30 m, which was divided into nine smaller areas of 10 m × 10 m. The device with the optimised parameters was placed in the centre of the small fertilisation area, and five fertiliser particles were then applied. According to the previous test, the distance between the fertiliser particle and soil was set at 200 mm, and the device was operated as described above. Then, the fertilisation depth was measured, and the average fertilisation depth of the five particles was taken as the fertilisation depth of this area.

Test results and analysis

The results of fertilisation depth are shown in Table 4. It can be seen that the fertilisation depth is relatively stable, ranging from 48.90 mm to 54.40 mm, with deviations of 0.6–8.8%. The paddy field is uneven after pulping and machine tillage, with the concave area storing water and the convex area drying out. Hence, the soil moisture content in the same area may be quite different. The variations in water content of the soil greatly affect the soil density and the mud resistance against the fertiliser particles, which will further influence the fertilisation depth. Therefore, errors in

fertilisation depth during the test may be ascribed to changes in soil moisture content. The soil moisture content of the test field was $37.00 \pm 2.60\%$, which can represent the moisture content of most paddy fields. Under this moisture content, the fertilisation depth by the device is ideal. However, for the paddy fields with other moisture contents, the predetermined fertilisation depth can be achieved by changing the compression amount of the spring.

TABLE 4. Field test results.

Area	Pre-set fertilisation depth (mm)	Actual fertilisation depth (mm)	Deviations (%)
1	50	52.6	5.2
2	50	54.4	8.8
3	50	53.1	6.2
4	50	53.7	7.4
5	50	48.9	2.2
6	50	52.9	5.8
7	50	50.3	0.6
8	50	52.8	5.6
9	50	49.6	0.8

Here, the field test did not involve the influence of the forward speed and body vibration of the tractor. In actual field fertilisation, these factors may also influence the fertilisation depth, but we believe that the impact distance, impact surface radian and fertiliser particle diameter have a constant influence on the fertilisation depth. Even though the forward speed of the tractor will make the fertilisation depth shallow, the kinetic energy of the fertiliser particle is still at a maximum and the fertilisation depth is still optimal, with a fertiliser particle diameter of 16.0 mm, impact distance of 56.5 mm and impact surface radian 29.6° . In addition, the non-contact fertilisation device is applied to rice water direct seeding. In this case, before rice planting and fertilisation, the soil should be cultivated with a pulping machine to ensure smooth and loose soil. As shown in Figure 11, the soil flatness is good. The soil density is relatively balanced after rotary tillage, and the non-contact fertilisation device can maintain good stability after being put into the field. Compared with rice drought direct seeding, rice water direct seeding will result in higher stability and smaller vibration of the tractor, which has less influence on the fertilisation process and depth (Chen et al., 2015). However, whether the above factors have significant impacts on the fertilisation depth should be determined in our future research.

CONCLUSIONS

1) By analysing the incident mud process of fertiliser particles, the factors influencing the impact mud resistance were determined. Through the theoretical analysis and finite element simulation of the fertilisation device, it was determined that the impact distance, the impact surface radian and the fertiliser particle diameter had the greatest impact on the fertilisation depth of the fertilisation device.

2) Single factor and orthogonal tests were carried out with impact distance, impact surface radian and fertiliser

particle diameter being test factors and fertilisation depth was the test index. The results showed that the order of the three factors on the depth of fertilisation was: fertiliser particle diameter > impact distance > impact surface radian. Taking the maximum fertilisation depth as the target, the optimal combination of working parameters was determined as follows: fertiliser particle diameter = 16.0 mm, impact distance = 56.5 mm, impact surface radian = 29.6° .

3) The field test was carried out in a paddy field with a water content of $37.00 \pm 2.60\%$. The field test showed that, when the pre-set fertilisation depth was 50 mm, the relative error between the pre-set value and the actual fertilisation depth was less than 8.8%, which can meet the requirements of side precision deep fertilisation for rice direct seeding.

ACKNOWLEDGEMENTS

This study was financially supported by a program of China's National Natural Science Foundation Project (No. 31901412), the National Key Technology R&D Program (No. 2017YFD0301300), the College Guidance Program (No. 2022GXYD004) and the Special Fund for Agro-scientific Research in the Public Interest (No. 201503136).

REFERENCES

- Chen C, Pan JJ, Lam SK (2014) A review of precision fertilization research. *Environmental Earth Sciences* 71(9):4073-4080. DOI: <https://doi.org/10.1007/s12665-013-2792-2>
- Chen LQ, Li Y, Cao CM, Zheng Q (2015) Optimization design for vibration reduction of micro planter and fertilizer machinery used in mountain area based on genetic algorithm. *Transactions of the Chinese Society of Agricultural Engineering* 31(03):17-22. DOI: <https://doi.org/10.3969/j.issn.1002-6819.2015.03.003>
- Dong XW, Li WK, Yi SJ, Zhu CY, Chen CH, Liu TX (2019) Research of intermittent fixed point and precision rice side deep fertilizing method and device design. *Journal of Heilongjiang Bayi Agricultural University*. DOI: <https://doi.org/10.3969/j.issn.1002-2090.2019.03.010>
- Jalalisendi M, Porfiri M (2018) Water entry of compliant slender bodies: Theory and experiments. *International Journal of Mechanical Sciences*. 149:514-529. DOI: <https://doi.org/10.1016/j.ijmecsci.2017.07.041>
- Lal R (2010) Enhancing crop yields in the developing countries through restoration of the soil organic carbon pool in agricultural lands. *Land Degradation & Development* 17(2):197-209. DOI: <https://doi.org/10.1002/ldr.696>
- Liu LY, Li HY, Zhu SH, Gao Y, Zheng XQ, X Y (2021) The response of agronomic characters and rice yield to organic fertilization in subtropical China: A three-level meta-analysis. *Field Crops Research* 263:108049. DOI: <https://doi.org/10.1016/j.fcr.2020.108049>
- May A (1952) Vertical Entry of Missiles into Water. *Journal of Applied Physics* 23(12):1362-1372. DOI: <https://doi.org/10.1063/1.1702076>

- May A, Woodhull JC (1948) Drag Coefficients of Steel Spheres Entering Water Vertically. *Journal of Applied Physics* 19(12):1109-1121. DOI: <https://doi.org/10.1063/1.1715027>
- Min J, Sun HJ, Wang Y, Pan YF, Herbert K, Zhao DQ, Shi WM (2021) Mechanical side-deep fertilization mitigates ammonia volatilization and nitrogen runoff and increases profitability in rice production independent of fertilizer type and split ratio. *Journal of Cleaner Production* 316(4):128370. DOI: <https://doi.org/10.1016/j.jclepro.2021.128370>
- Shen C, Yu PY, Wang TL, Chen NZ (2022) A CFD based Kriging model for predicting the impact force on the sphere bottom during the early-water entry. *Ocean Engineering* 243:110304. DOI: <https://doi.org/10.1016/j.oceaneng.2021.110304>
- Sui YT, Zhang AM, Ming FR, Li S (2021) Experimental investigation of oblique water entry of high-speed truncated cone projectiles: Cavity dynamics and impact load. *Journal of Fluids and Structures* 104:103305. DOI: <https://doi.org/10.1016/j.jfluidstructs.2021.103305>
- Wan L, Xie DP, Li Y, Chen LQ (2020) Design and Experiment of Roller Hole Fertilizer Application between Corn Rows. *Transactions of the Chinese Society for Agricultural Machinery* 51(11):64-73. DOI: <https://doi.org/10.6041/j.issn.1000-1298.2020.11.007>
- Wang C, Li HW, He J, Wang QJ, Cheng XP, Wei ZC, Li JX (2019) Effect of incident angle on wheat soil-ripping parameters by pneumatic seeding. *Transactions of the Chinese Society of Agricultural Engineering* 35(16):32-39. DOI: <https://doi.org/10.11975/j.issn.1002-6819.2019.16.004>
- Wang C, Li HW, He J, Wang QJ, Lu CY, Wang JX (2020) Design and Experiment of Pneumatic Wheat Precision Seed Casting Device in Rice-wheat Rotation Areas. *Transactions of the Chinese Society for Agricultural Machinery* 51(05):43-53. DOI: <https://doi.org/10.6041/j.issn.1000-1298.2020.05.005>
- Wang JF, Gao GB, Weng WX, Wang JW, Yan DW, Chen BW (2018b) Design and Experiment of Key Components of Side Deep Fertilization Device for Paddy Field. *Transactions of the Chinese Society for Agricultural Machinery* 49(06):92-104. DOI: <https://doi.org/10.6041/j.issn.1000-1298.2018.06.011>
- Wang JF, Shang WH, Weng WX, Wang JW, Wang Q, Chen XS (2021) Design and Experiment of Disc Ejection Type Paddy Field Side Deep Fertilization Device. *Transactions of the Chinese Society for Agricultural Machinery*, 2021, 52(06):62-72. DOI: <https://doi.org/10.6041/j.issn.1000-1298.2021.06.007>
- Wang JW, Li SW, Zhang Z, Li QC (2018a) Design and experiment of electrical drive side deep hill-drop fertilization system for precision rice hill-direct-seeding machine. *Nongye Gongcheng Xuebao/Transactions of the Chinese Society of Agricultural Engineering* 34(8):43-54. DOI: <https://doi.org/10.11975/j.issn.1002-6819.2018.08.006>
- Wen XL, Liu PQ, Qu QL, Hu TX (2020) Impact of wedge bodies on wedge-shaped water surface with varying speed. *Journal of Fluids and Structures* 92:102831. DOI: <https://doi.org/10.1016/j.jfluidstructs.2019.102831>
- Wu ZY, Zhang CC, Wang J, Shen C, Yang L, Ren LQ (2020) Water entry of slender segmented projectile connected by spring. *Ocean Engineering* 217:108016. DOI: <https://doi.org/10.1016/j.oceaneng.2020.108016>
- Yang LW, Chen LS, Zhang JY, Liu HJ, Sun ZC, Sun H, Zheng LH (2018) Fertilizer sowing simulation of a variable-rate fertilizer applicator based on EDEM-ScienceDirect. *IFAC-PapersOnLine* 51(17):418-423. DOI: <https://doi.org/10.1016/j.ifacol.2018.08.185>
- Zhao C, Huang H, Qian ZH, Jiang HX, Liu GM, Ke XU (2020) Effect of side deep placement of nitrogen on yield and nitrogen use efficiency of single season late japonica rice. *Journal of Integrative Agriculture* 19:2-17. DOI: [https://doi.org/10.1016/S2095-3119\(20\)63362-7](https://doi.org/10.1016/S2095-3119(20)63362-7)
- Zhong XM, Peng JW, Kang XR, Wu YF, Luo GW, Hu WF, Zhou X (2021) Optimizing agronomic traits and increasing economic returns of machine-transplanted rice with side-deep fertilization of double-cropping rice system in southern China. *Field Crops Research* 270:108191. DOI: <https://doi.org/10.1016/j.fcr.2021.108191>
- Zuo XJ, Wu GW, Fu WQ, Li LW, Wei XL, Zhao CJ (2016) Design and experiment on air-blast rice side deep precision fertilization device. *Transactions of the Chinese Society of Agricultural Engineering*. DOI: <https://doi.org/10.11975/j.issn.1002-6819.2016.03.003>